

## Comparing Direct and QL Calculation of ICRF Diffusion Coefficients

R.W. Harvey<sup>\*</sup>, Yu. Petrov<sup>\*</sup>, E.F. Jaeger<sup>#</sup>, L.A. Berry<sup>#</sup>, D.B. Batchelor<sup>#</sup>,  
P.T. Bonoli<sup>+</sup>, J.C. Wright<sup>+</sup>

<sup>\*</sup> *CompX, P.O. Box 2672, Del Mar, CA 92014-5672, USA*

<sup>#</sup> *Oak Ridge National Laboratory, Oak Ridge, USA*

<sup>+</sup> *MIT Plasma Science and Fusion Center, Cambridge, USA*

**Keywords:** RF Heating, Fokker-Planck, plasma simulation

**PACS:** 52.50.Qt, 52.65.Ff, 52.65.-y

The DC diffusion coefficient calculator numerically integrates the orbits of ions launched from tokamak midplane points, equispaced in initial gyro-phase about given gyro-center and also in toroidal length along a given RF mode wavelength, and averages the resulting square of the velocity changes after one (or more) poloidal circuits in combined tokamak equilibrium and RF full wave fields from the AORSA full-wave code[1] to obtain the diffusion coefficient. This is carried out for a 3D array  $(v_{\parallel}, v_{\perp}, R)$  of initial conditions, giving the six independent RF diffusion coefficients in 3D constant-of-motion space. The method follows the formalism of Refs. [2,3]. For comparison, we have the zero-banana-width RF diffusion coefficients calculated in the AORSA code[1]. Comparison is more directly achieved by subtracting off the perpendicular guiding center drifts using a fictitious force in the Lorentz equation,  $\mathbf{F}_{\perp} = \mathbf{v}_{gc} \times \mathbf{B}$ . This removes the finite banana width effects, but leaves correlation, finite gyro-radius, and other effects. The integration of (64 radii) x (128  $v_{\perp}$ ) x (256  $v_{\parallel}$ ) x (8 gyro-phase) x (8 toroidal angle) starting positions (13.4M Lorentz orbits) is well-parallelized and takes 1 hour on 2048 cores; these global calculations are enabled by recent advances in supercomputing[4].

The DC code is similar to the MOKA code[5], but has been coupled to the CQL3D Fokker-Planck code[6] and AORSA to obtain a time-dependent, noise-free solution to the ICRF heating problem across the whole plasma width.

For a canonical C-Mod, 4% minority H,  $T_e = T_i = 2.9$  keV case[7], [Figure 1](#) shows that good agreement is obtained between radial ICRF power absorption profiles calculated with [DC\\_W0](#) “zero-banana-width” DC diffusion coefficients, and AORSA calculated Kennel-Engelmann[8] diffusion coefficients, particularly when the distribution is nearer isotropic, to time  $t = 0.5$  msec. In this test case, the fundamental-H cyclotron resonance pass near the magnetic axis. Also shown in [Figure 1](#) is the power absorption profile [DC\\_W1](#) resulting from finite-banana-width (i.e. unmodified Lorentz) DC gyro-orbits, for which ions are started at radial positions such that their bounce-averaged radial position corresponds to the given radial coordinate values (with adjustment near the magnetic axis for axis-encircling orbits which can have gyro- and banana-widths greater than the distance to the magnetic axis). Power absorption is calculated as the zero-banana-width flux-surface average of

$\int d^3u (1/2) m u^2 \left| \frac{\partial f_{ion}}{\partial t} \right|_{RF}$ , where  $\left| \frac{\partial f_{ion}}{\partial t} \right|_{RF}$  is the diffusion term resulting from the rf velocity space diffusion coefficients operating on the ion distribution. Figure 1(d) shows “specific” rf power density versus velocity, obtained by integration the velocity-space pitch angle, thus also showing good agreement in detail in velocity space.

The agreement between DC and AORSA zero-banana- width power profiles in Fig. 1(a) and (b) is good, less that 20% difference in total power, in view of the differences in method of calculation. The RF velocity-space “kicks” are completely correlated in DC, but are randomly phased for each resonance in AORSA. Moreover, there is no accounting for higher order tangent resonant effects. However, the rf diffusion coefficients are quite different, as shown in Figure 2(a) from DC and 2(b) from AORSA. Both figures are on the same scale. The relatively large variation in 2(a) compared to 2(b) is due to correlations between multiple passes of the cyclotron layer, which in the present case passes vertically very near to the plasma magnetic axis.

Figure 3 illustrates the reinforcement or cancellation of the velocity space kicks which occur due to correlation between two resonant interactions using a simplified model built on an ion cyclotron damping model in Stix's ICRF paper[9]. Plasma with circular flux surfaces is assumed, with toroidal magnetic field varying as  $R^{-1}$  and cyclotron resonance through the magnetic axis. Stix's equation for the cyclotron

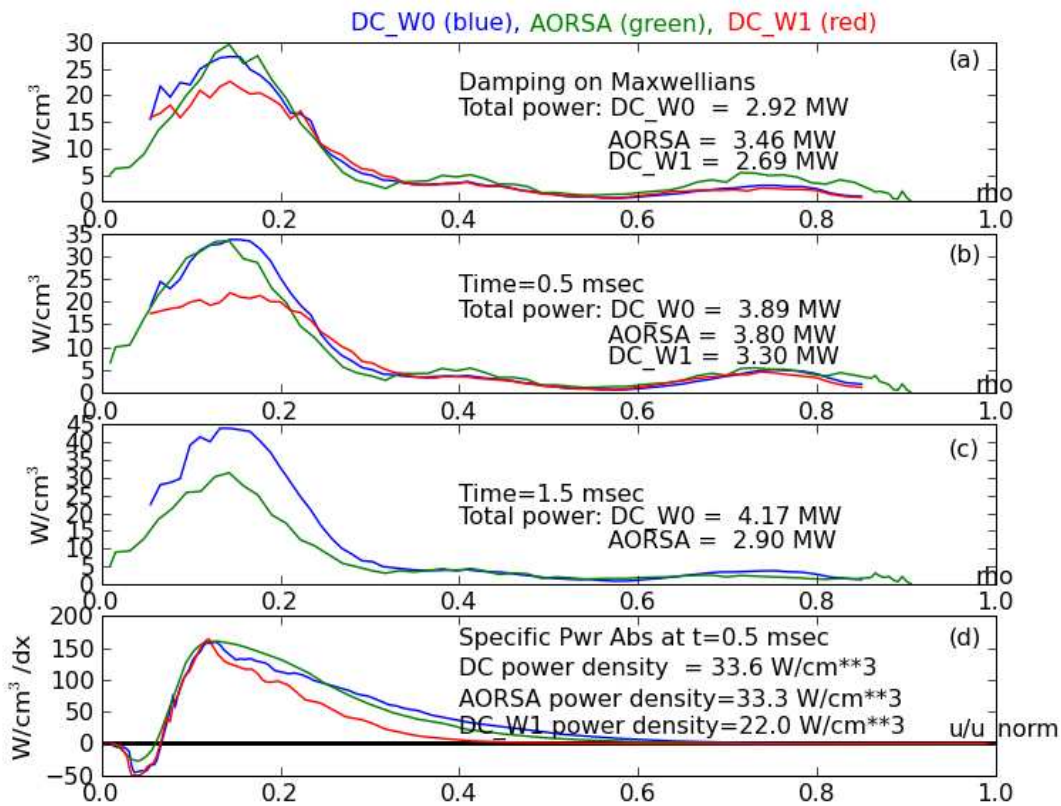


Figure 1. (a)-(c) Minority-H power deposition versus radius for C-Mod ICRF test case. DC\_W0 refers to diffusion coefficients from DC with zero-orbit-width option, AORSA uses Kennel-Englemann coefficients, and DC\_W1 uses finite-width orbits from DC. (d) Specific power density per  $dx$ , where  $x$  is normalized velocity, integrated in pitch coordinate,  $\rho=0.14$ .

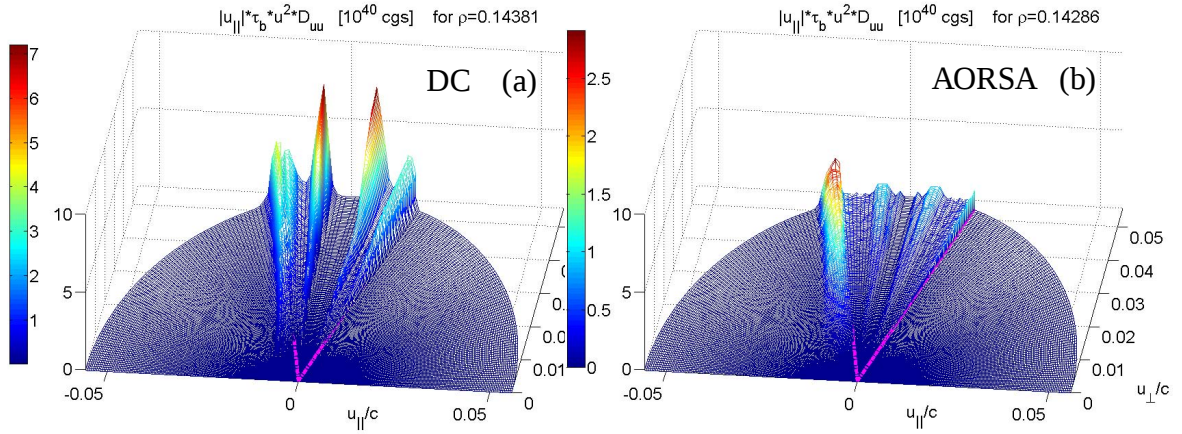


Figure 2. The  $D_{uu}$  related RF diffusion coefficients calculated in (a) from zero-orbit-width DC, and in (b) from AORSA. Substantial differences in strength are due to correlations in DC.

interaction is  $\frac{du_{\perp}}{dt} + i\Omega(t)u_{\perp} = \frac{q}{m}E_{+}\exp(-i\omega t)$ , where  $u_{\perp} \equiv u_x + iu_y$  is the complex perpendicular velocity, and  $\Omega(t)$  is the local cyclotron frequency along the ion orbit. An approximate solution given by Stix for one pass through resonance is

$$u_{\perp}(t) = (u_{\perp}(-\infty) + U)\exp(-i\int_{-\infty}^t \Omega dt), \text{ where } U \equiv \frac{q}{m}E_{+}\left(\frac{2\pi i}{d\Omega/dt}\right)^{1/2}.$$

From this, we find an expression for the phase average diffusion coefficient for a single pass through the resonance region which agrees within small numerical error with what is obtained by numerical integration of the above differential equation for  $u_{\perp}$ .

In Figure 3(a), we compare numerically determined phase average diffusion after two correlated passes of the resonance region, with the analytic expression for two uncorrelated passes as will be obtained with quasilinear theory. This shows that the correlations for two resonances double the maximum diffusion coefficient, relative to the uncorrelated interaction with two resonances. However, the  $\sin(\theta_0)$ -weighted integrals over pitch angle of the diffusion coefficient, proportional to rf power absorption on an isotropic distribution, are equal to within numerical error. The same general result is obtained with four successive resonances, as happens for trapped particles during one poloidal transit. Thus, this model appears to explain both the large variation of the DC diffusion coefficients relative to AORSA shown in Figure 2, and the excellent agreement between the power absorption in Figure 1 at small times in solution of the Fokker-Planck equation. The correlations shift the diffusion coefficient around in pitch angle, but for an isotropic ion distribution the power absorption is unaffected.

A concern in these calculations was the effect of starting the ion orbits within the rf fields, giving fictitious “diffusion” due to the non-resonant fields. Figure 3(b) with the simplified model but with the  $E^+$ -field uniform in the poloidal cross-section, indicates this is not a substantial affect, particularly when averaged over pitch angle.

With additional Fokker-Planck time steps, the pitch angle variation of distribution functions becomes different in the DC and AORSA diffusion coefficient cases at C-Mod ICRF power levels, and thus differences develop in the power absorption profiles. Enhanced distribution function tails at pitch angles of correlated RF “kicks”

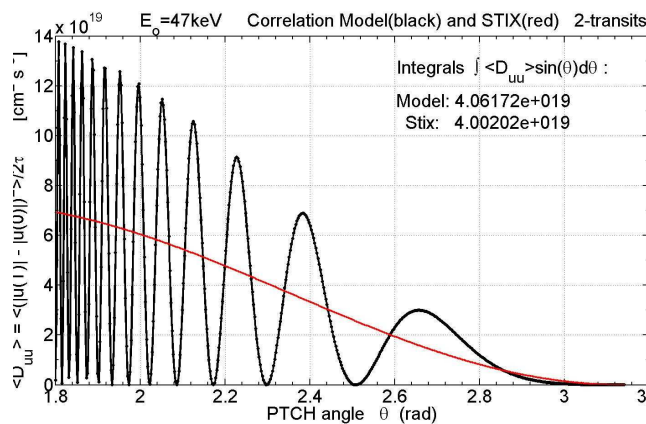


Fig. 3a. Gyro-phase average diffusion coefficient after two transits of resonant surface. The  $E^+$ -field peaks near the resonance surface, which passes through the magnetic axis.

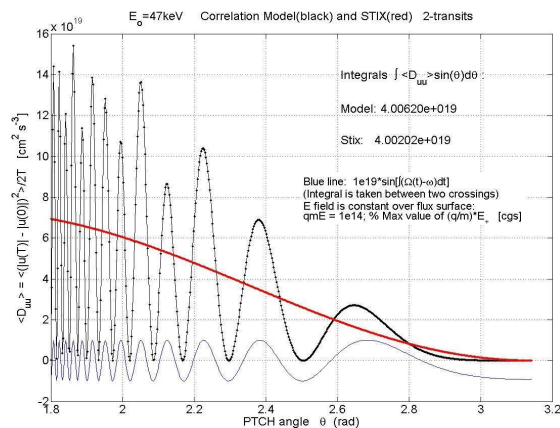


Fig 3(b). Same as Fig. 3(a), except that the  $E^+$ -field is constant across the poloidal cross-section, indicating little change in results due to starting particles in the non-resonant fields.

reasonable first approximation. This approach is being further explored.

Research supported by USDOE SciDAC awards ER54649, ER54856, and DC-AC-5-00OR22725.

## REFERENCES

1. E.F. Jaeger, L.A. Berry, *et al.*, Nucl. Fusion **46**, (2006) S397-S408.
2. A. Kaufman, Phys. Fluids **15**, 1063 (1972).
3. L-G. Eriksson and P. Helander, Phys. Plasmas **1**, 308 (1994).
4. This research used resources of the National Energy Research Scientific Computing Center, supported by the Off. of Science of the U.S. Dept. of Energy Contract DE-AC02-05CH11231.
5. V. Bergeaud, F. Nguyen, A. Becoulet and L-G. Eriksson, Phys. of Plasmas **8**, 139 (2001).
6. R.W. Harvey and M.G. McCoy, "The CQL3D F-P Code", IAEA TCM, Montreal (1992).
7. A. Bader, P. Bonoli, *et al.*, Bull. Amer. Phys. Soc., (AIP, NY, 2008), Paper PP6.00100.
8. C. Kennel and F. Engelmann, Phys. Fluids **9**, 2377 (1966).
9. T.H. Stix, Nucl. Fus. **15**, 737 (1975).
10. E.F. Jaeger, L.A. Berry *et al.*, Phys. Of Plasmas **15**, 072513 (2008).

increase the absorption, as in Figure 2(c). On the other hand, correlation effects are probably exaggerated in the present single-toroidal-mode case. In ITER, considering a broad spectrum of toroidal ICRF modes, Jaeger[10] has shown strong single-pass absorption of ICRF in a D-T-He plasma, giving the result that the rf is very localized in toroidal angle. In this situation, the ions can toroidally precess out of the rf region in one bounce, greatly reducing correlation effects. Correlation, and loss of correlation are being examined further with DC.

Returning to the red curves in Figure 1, they indicate substantial radial spreading of the power deposition due to finite-banana-width effects. Full compatibility between DC coefficients and a Fokker-Planck code requires a finite-orbit width code. With small orbit-width relative to plasma radius, assigning the orbits to their bounce-average radius, and balancing with the zero-orbit width collision calculations provides a